19e Journées de l'Hydrodynamique
26 – 28 novembre 2024, Nantes

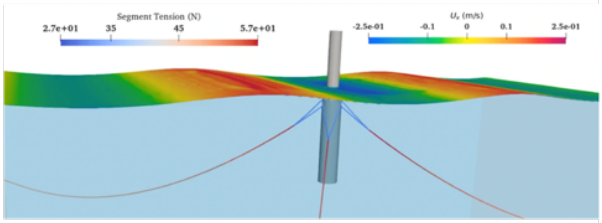

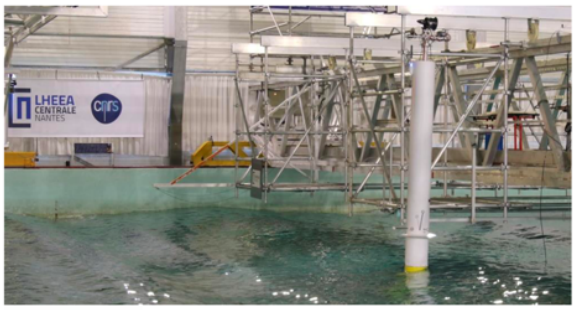

EXPERIMENTAL INVESTIGATION OF THE WAKE DEVELOPMENT AROUND A COUNTER-ROTATING TWIN VERTICAL AXIS TIDAL TURBINE

Y. SAOULI[1,2], C. HINARD[1], B. GAURIER[1], G. GERMAIN[1], G. MAURICE[2]
yanis.saouli@ifremer.fr ; gregory.germain@ifremer.fr

[1]Laboratoire Hydrodynamique Marine, Ifremer, Boulogne-sur-Mer
[2]Hydroquest SAS, Meylan

Résumé

Cette étude se concentre sur l'analyse expérimentale du développement du sillage des turbines OQ 2.5 d'Hydroquest, à double axe vertical bi-rotors contrarotatifs. Une maquette échelle 1/20 est soumise à un écoulement incident établi dans le bassin à houle et courant de l'Ifremer. Des mesures LDV et PIV permettent d'étudier la zone d'induction ainsi que le sillage proche et lointain de la turbine. Les résultats montrent que la géométrie de la turbine et de la fondation entraîne un fort contournement de l'écoulement. La rotation des rotors génère des zones de recirculation en aval, source d'un mélange important dans le sillage proche. Les résultats montrent également que la largeur du sillage varie peu avec la distance en aval, tandis que la hauteur du sillage diminue fortement lorsque l'on s'éloigne de la machine.

Summary

This study focuses on the experimental analysis of the wake development of Hydroquest's OQ 2.5 turbines, with counter-rotating twin vertical axis bi-rotors. A 1:20 scale model is subjected to an established incident flow in Ifremer's wave and current flume tank. LDV and PIV measurements make it possible to study the induction area as well as the near and far wake of the turbine. Results reveal that the geometry of the turbine and its foundation induces flow deviation. The rotation of the rotors generates recirculation zones downstream of the turbine, resulting in significant mixing in the near wake. The results also show that the wake width varies little with the distance downstream of the turbine, while the wake height is significantly lessened with increasing distance from the machine.

I – Introduction

The successful commercialization of vertical axis tidal turbines (VATTs) hinges on a comprehensive understanding of their operations. In the context of the FloWatt project, Hydroquest is developing a new generation of VATTs (OQ 2.5) adapted to the challenging environmental conditions of the Raz-Blanchard area [1]. These innovative machines promise significant advancements in harnessing tidal energy, but their deployment on a commercial scale requires meticulous investigation of their behaviour [2].

Understanding the wake dynamics of the tidal turbines is crucial for several reasons. The performance and efficiency of the turbines could be directly influenced by the characteristics of nearby turbines, including generated turbulence intensity, velocity deficit and wake recovery length [3]. Such interactions can lead to high fluctuations in power output and influence the structural integrity and lifespan of the turbines. Therefore, optimizing the placement of multiple turbines within a tidal farm is necessary to minimize energy losses and mechanical stresses [4, 5], ensuring sustainable and efficient energy production.

Experimental studies can provide essential insights into these wake aspects, and also offer data to validate and refine computational models [6]. This approach enhances the fidelity of CFD models making it possible to establish machines' behaviour under a wide variety of conditions, but also informs design improvements and operational strategies. An experimental approach (Fig. 1) to study the wake development of Hydroquest's turbines is then mandatory for their fruitful commercial deployment.

FIGURE 1 – 1:20 scale model disposed on the floor of the Ifremer flume tank.

In this work, experimental tests carried out in the Ifremer wave and current flume tank for the turbine wake characterisation are presented. The results concerning the mean wake development for the flow facing the turbine at its optimum operating point are discussed. In the following, the impact of the machine on the upstream flow is first assessed. Then, the flow behaviour around the whole model is analysed and the far wake is investigated.

II – Experimental setup and input characteristics

II – 1 1:20 model characteristics

The model studied is the $1{:}20^{th}$ prototype of the 2.5 MW-rated machines (Fig. 1) planned to be deployed for the FloWatt project. This model, named OQ 2.5, is composed of two vertical axis rotor columns, also made of two levels of rotors with a 60° phase difference between them. Its dimensions are defined in order to respect the geometric similarity in the tank, and therefore to respect the ratio between the height of the machine and the height of the water column.The model is H_m= 1.010 m high, for a width with

rotors of $w_m = 1.270$ m. The rotors are $H_b = 0.315$m and $R = 0.235$ m respectively for the height and the radius. The distance between the bottom plate and the top plate holding the rotor columns determines the turbine height : $h_m = 0.83$ m. The foundation is composed of three lested arms, fixed to the anchor base. The arm going upstream is placed along the flow axis in config F.
The driving system is installed in blocks located under the axis of the two columns, comprising a 26:1 geared motor and a torquemeter. The system makes the two columns rotate to a rotational set speed ω. The reference area is defined here as the blue surface on the Fig.2 (right), representing the projected capture area $S_{ref} = h_m \times w_m$. An equivalent diameter D_e is derived from this surface, defined from the IEC norm : $D_e = \sqrt{\frac{4S_{ref}}{\pi}}$, which is used to transform a non-circular cross-section machine into an equivalent device with a circular cross-section. D_e and U_0 are here considered as the reference length and velocity for normalising studied parameters.

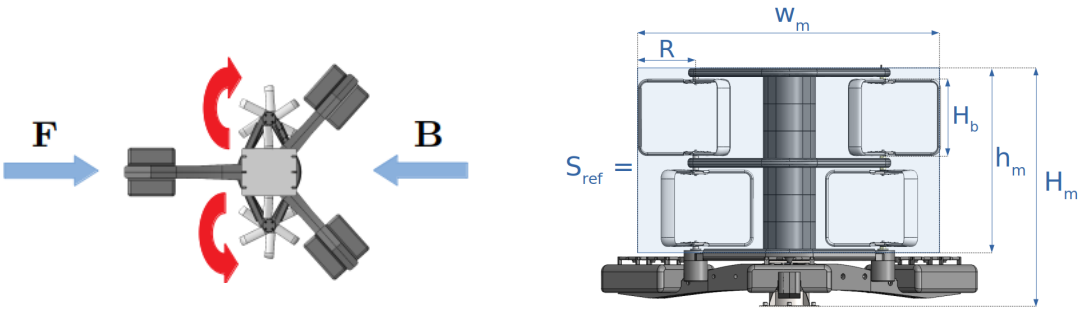

FIGURE 2 – Left : main studied configurations of the model (Facing [F] and Back [B]). In this paper, only the config F is studied. The red arrows indicate the rotation direction of both rotor columns. Right : reference surface S_{ref} taken as the projected capture area of the turbine.

II – 2 Sea conditions modelling in the flume tank

The OQ 2.5 model is tested in the wave and current circulating tank of IFREMER situated in Boulogne-sur-Mer (France). The test section is 18 m long × 4 m wide × 2 m deep (see Fig. 3). The incoming flow (U_0, V_0, W_0) is assumed to be constant and steady, with the imposed velocity : U_0= 1.0 m/s and $V_0 = W_0 = 0$ m/s. The three instantaneous velocity components are denoted (U, V, W) along the (x, y, z) directions respectively, with x the main flow direction. The model is placed at the centre of the tank, with the x-origin set at its centre, z = 0 corresponds to the tank floor. The model is centred in the span-wise direction of the tank, with the span-wise origin (y=0) set to the centre of the model, and so of the tank. Thanks to a grid combined with a honeycomb placed at the inlet of the working section, a low turbulence intensity $TI_0 = 1.5\%$ is reached [7] and the boundary layer height, calculated as follows $\delta_{95} = 0.95 \times U_0$, is equal to $\delta_{95} \approx 0.25$ m. The expression of the flow velocity components follows the Reynolds decomposition :

$$U_i(t) = \overline{U_i} + u_i'(t) \tag{1}$$

with $\overline{U_i}$ the mean component and $u_i'(t)$ the fluctuating part of the flow velocity.
With the geometric similarity, the Froude similarity is respected :

$$F_r = \frac{U_0}{\sqrt{g.(h_t - H_m)}} = 0.32 \tag{2}$$

For this study, the Reynolds number $R_e = \frac{U.D_e}{\nu}$ in the tank is of the order of 10^5, which is about 100 times lower than in full-scale conditions.

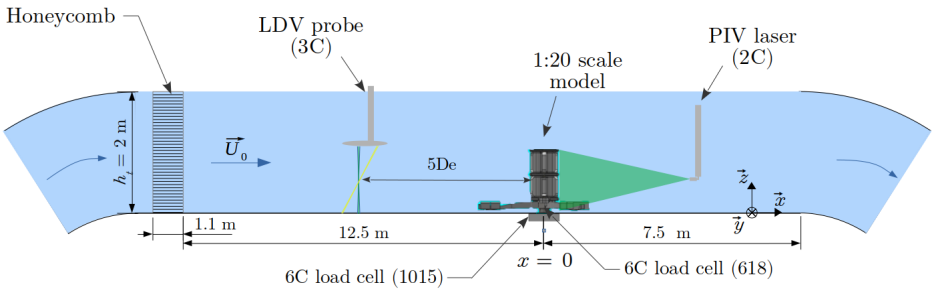

FIGURE 3 – Schematic description of the flume tank during the tests.

II – 3 Measurement tools and planes

In order to assess the flow behaviour at different positions in the tank, the current velocity is measured using the Dantec 3-Components Laser Doppler Velocimeter (LDV-3C) in non-coincident mode, so that each velocity component is measured independently from the others. The acquisition time is 3 minutes per run to guarantee the convergence of mean and standard deviation velocity.

LDV measurements follow the coarse mesh presented in Fig. 4 (bottom left) for different x positions (Fig. 4, top). The symmetry of the flow was verified by symmetrical profiles behind the rotor columns at x/D_e=1 (Fig. 4, bottom right). Mean velocity components and standard deviations are found similar on the whole water column between the profiles, confirming the validity of this mesh consideration. Other experimental studies such as [4], with the interaction of two vertical axis rotors, corroborate this proposition. Given that symmetry has been verified, the maps based on the LDV measurements will be mirrored symmetrically around the two columns (section V).

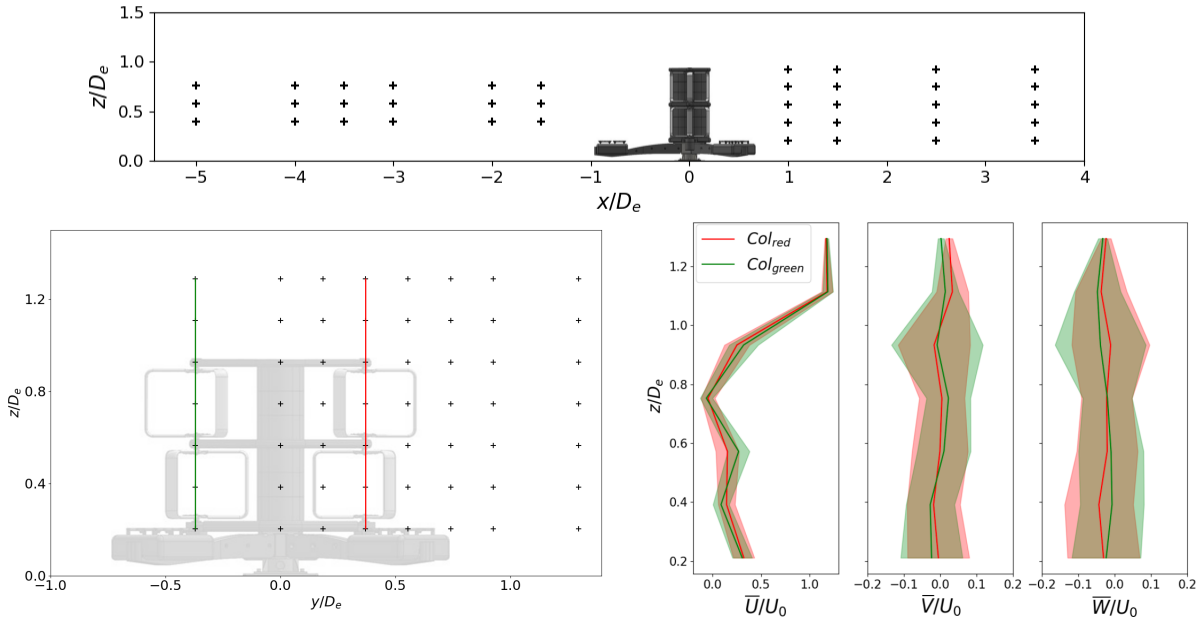

FIGURE 4 – Top : LDV measurement points (black crosses) in the tank, to the half rotor y-position. Upstream, measurements are made for half-rotors y-position and y=0. Bottom : symmetrical profiles behind the rotors showing the same trends on the water column.

The flow behaviour close to the machine is evaluated using PIV technique. The measurements are made using cameras HisenseZyla USB 5.5, with a greyscale coding parameter

of 16 bits for each pixel. Planes deployed vertically (see Fig. 5, top) are 875 mm × 1050 mm with a spatial resolution of $dx = dz = 13$ mm. For the ones deployed horizontally (see Fig. 5,bottom), dimensions are 580 mm × 695 mm, with $dx = dz = 9$mm. For the horizontal PIV measurements, blade passages are hidden using a dynamic masking when calculating average quantities.

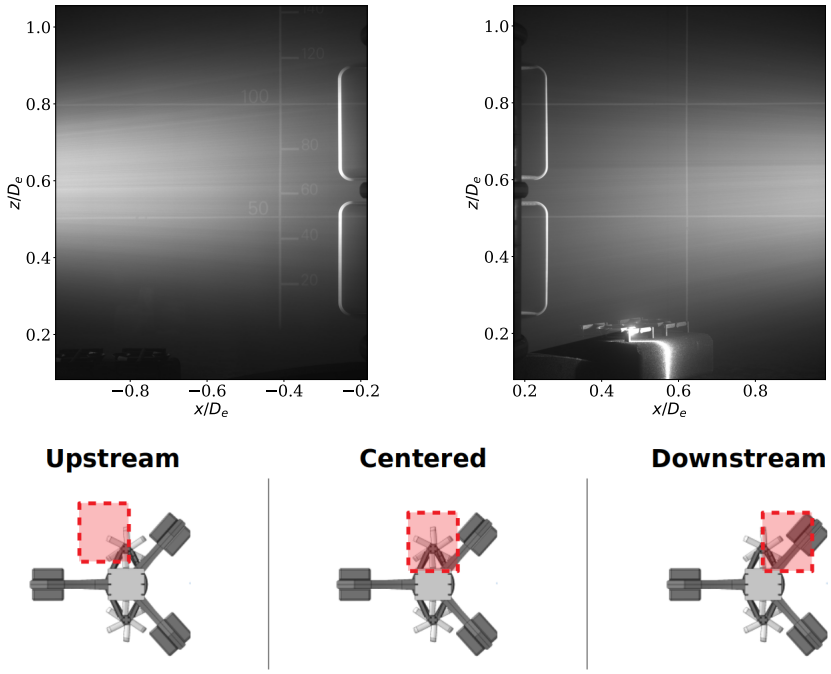

FIGURE 5 – Top : vertical PIV measurement planes around the model (y-position : half rotor column). Bottom : horizontal PIV measurement planes positions around the model (z-position : mid-height of the upper rotor). Same results are observed for both stages of rotors.

From -5D_e upstream to 3.5D_e downstream of the turbine, LDV and PIV measurements can help to understand the flow behaviour in interaction with the turbine.

III – Effects on the flow upstream of the machine

Studying the upstream effect of an immersed turbine is crucial because the turbine acts as a dynamic obstacle which significantly influences the incident flow velocity profile. Investigation at the optimum operating point of the model would help to deepen knowledge on turbine's induction effects.

Fig. 6 shows the mean U-velocity evolution for six different locations upstream from the turbine's projected capture area. As the values are normalised by the U-velocity at the furthest position (x/D_e = -5), it can be seen that the flow streamwise velocity component profiles converge from 3D_e upstream of the turbine, considering a 1% difference criterium based on LDV measurement accuracy.

Upstream effects are also studied in the near-machine field using PIV measurements. Moving closer to the model, the flow behaviour becomes highly disturbed, as highlighted by the vertical profiles of the Fig. 7. Acting as an obstacle, the flow streamwise component decreases by almost 20% near the moving rotors comparing profiles at x=−1.5D_e and x=−0.37D_e. Conversely, vertical velocity components absolute values increase at the top and bottom plates z-positions, reflecting the flow bypassing around the rotor column.

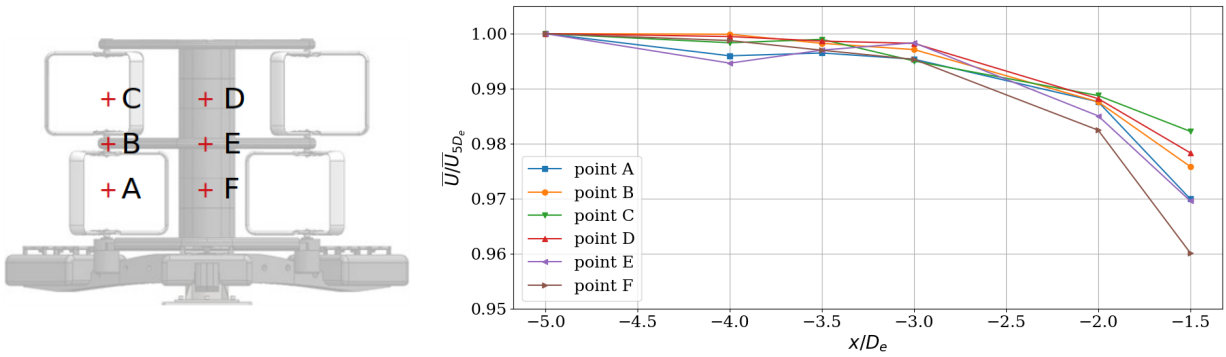

FIGURE 6 – Evolution of the upstream flow through the velocity component U, depending on the upstream x-position. Each velocity is normalised by the U-value measured at $x = -5De$ and at the same (y,z) position. The study of the W-value provides the same results.

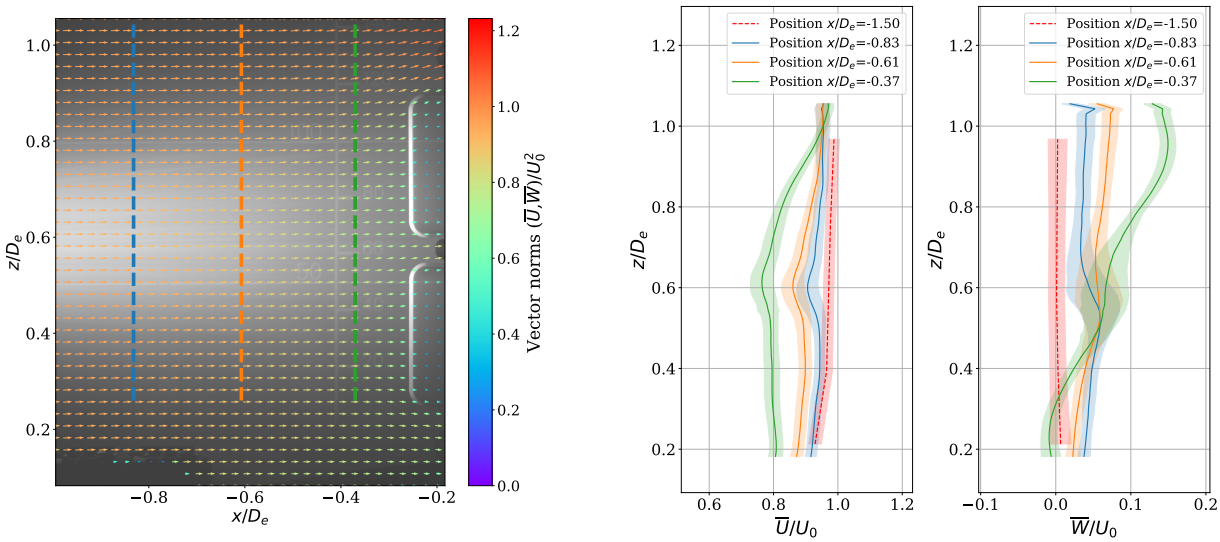

FIGURE 7 – Flow disturbances due to the presence of the machine (mean velocity + standard deviation from PIV acquisitions). The red profile is obtained through the LDV measurements far upstream (to x/D_e=-1.5). The outlier values at mid-height of the profiles ($z/D_e \in [0.55; 0.60]$) are caused by the laser source generating a disturbance in the flow.

Horizontal PIV measurements presented in Fig. 8 reveal that the upstream effect of the rotors manifests as a decrease of the streamwise component, consistent with the vertical profiles. The velocity reduction is more pronounced near the central pillar of the structure, although a slight decrease of $\overline{U}$ is observed for $y/D_e \geq 0.6$. This trend is explained by the flow bypassing the turbine and the flow-machine interaction ahead of the rotors relating to energy harvesting. The observations are similar to those made by CFD in the context of interaction between two vertical axis rotors [5]. The upstream velocity is greatly reduced along the axis of the two rotors but accelerates outside the capture surface, and is also contrained on the other side due to the presence of the central pillar. In our case, the flow exhibits a pronounced lateral acceleration, with the passage of the blades. The bypass results in a significant increase in the lateral flow component around the disc representing the rotor position, with $\overline{V}$ reaching almost $0.5U_0$ near the rotor. The large extent of the lateral velocity component in the plane and the specific direction of the column rotation

suggest that the rotor tends to extend the wake outside of the blockage zone.

In this section, the decrease in the upstream streamwise velocity component and the evolution of the upstream lateral flow demonstrate that the turbine in operation has a significant effect on the incident flow. Additional elements of the resulting interaction on the flow close to the machine are presented in the following section.

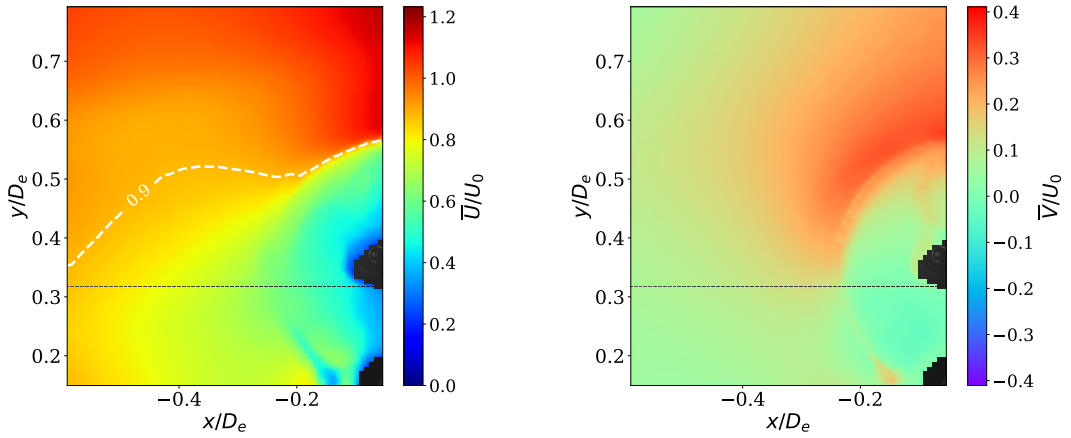

FIGURE 8 – Horizontal PIV measurements upstream of the rotor column. Mean velocity components $\overline{U}$ and $\overline{V}$ are displayed. The white dot lines on $\overline{U}$ maps define the contour for which $\overline{U}/U_0$=0.9.

IV – Near-machine flow behaviour

To further explore the flow-machine interaction, the flow behaviour is analyzed around the rotor column and in the near-wake region of the model.

First of all, the horizontal planes in Fig. 9 (top) confirm earlier findings, showing a lower $\overline{U}$ value upstream of the rotor ($0 \geq x/D_e$). At the interface of the rotor swept area, the lateral flow component $\overline{V}$ shows significant values, reaching up to 30% of U_0. Downstream of the rotor, a high gradient in $\overline{U}$ differentiates an external region where $\overline{U} \geq 0.9U_0$, and a low $\overline{U}$ velocity zone related to the rotor wake. In this wake area, a notable velocity deficit is observed, indicating that the turbine at its optimum operating point has extracted an important part of the flow's energy.

In contrast, the external region downstream of the rotor shows an acceleration of the flow, with streamwise velocities exceeding the incident velocity. Initially, at the turbine (x=$0D_e$), the external velocity is about $1.08U_0$. Further downstream, based on the maps of the Fig. 9 (bottom), the overspeed is settling around $1.25U_0$.

Additionally, the Fig. 9 (bottom) highlights the lateral expansion of the rotor wake. The flow emerging from the rotors is directed outward from the rotor plane, guided by the $\overline{U}$ gradient and characterized by a generally positive $\overline{V}$ component in the external region. This observation aligns with numerical results from RANS-based models [8], suggesting that the wake spreads laterally for this direction of rotation.
However, the lateral velocity component $\overline{V}$ is directed towards the central pillar when the blade moves inward. It indicates that the rotor wake is thus constrained by the external area, as highlighted by the $\overline{U}$ gradient, and by the central pillar wake extended downstream.
Considering the geometric and Froude similarity, it is also possible to study the impact that the machines would have on the entire water column. To do so, complementary LDV measurements were conducted (see Fig. 10, left). Measurements show that an overspeed

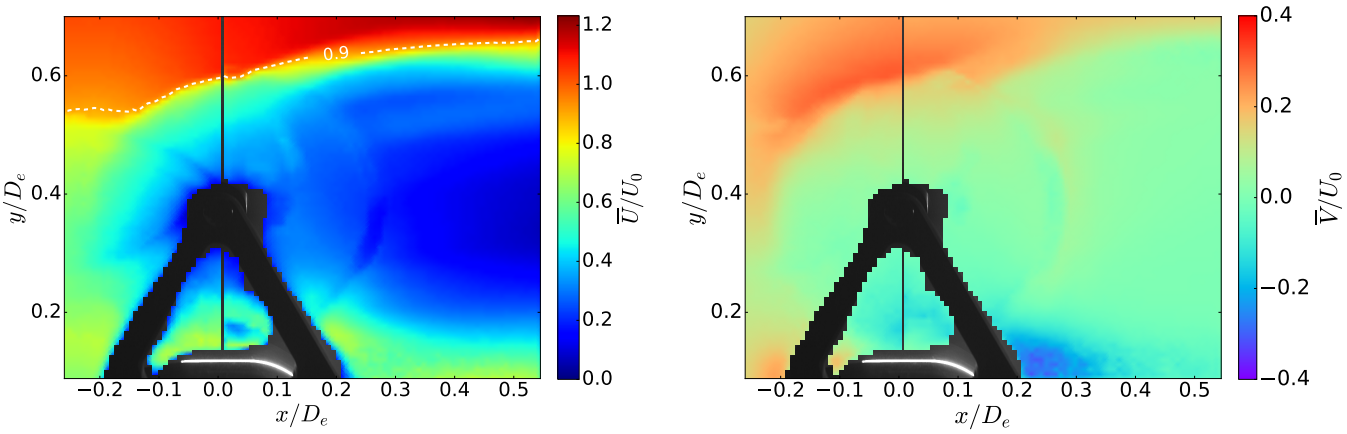

FIGURE 9 – Horizontal PIV measurements centered around a rotor column. Mean velocity components $\overline{U}/U_0$ (left) and $\overline{V}/U_0$ (right) are displayed. The white dot lines define the contour for which $\overline{U}/U_0 = 0.9$. The disc described by the blades passage can be discerned.

begins at the front upper plate of the turbine and then expands to the surface. The presence of the machine alters the flow velocity, which is accelerated by 10% to 20% in the upper part of the water column.

To complete this analysis, vertical PIV measurements were taken downstream of the rotor column, as shown in Fig. 10 (right). One can see the persistence of the overspeed outside the wake, for $z/D_e \geq 1$. The streamwise velocity deficit is also noticeable in the wake, with a streamwise velocity component $\overline{U}/U_0$ approaching 0. Moreover, the streamlines reveal a recirculating zone approximately $1D_e$ downstream of the upper rotor only. The wake caused by the flow around the central plate develops in the flow, moving downwards. The wake of the lower rotor is then constrained by both the central plate's wake and the machine's foundation arm, which seems to be a condition of non-appearance of the recirculating zone. As a complement, the study of the vertical velocity component $\overline{W}$ shows an overall trend of the wake to move downwards.

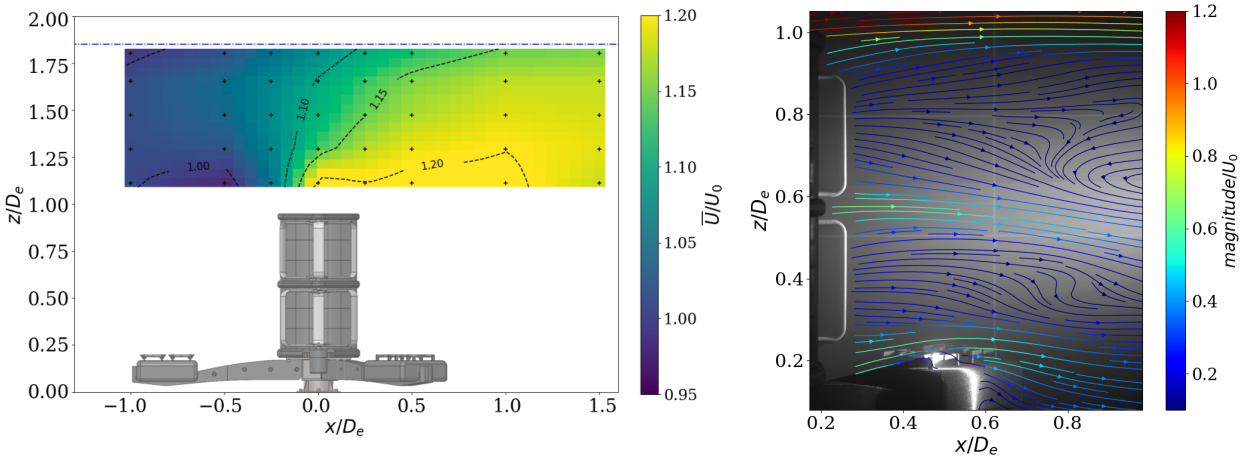

FIGURE 10 – Left : investigation of the overspeed over the whole structure using LDV measurements, with U velocity peak of $1.25U_0$. Right : streamlines map with normalised vector magnitude, downstream from half-rotor column. The map presents the rotors' wake influenced by the geometry of the turbine, and a part of the external region (top).

After the description of the global near-wake, the characterisation of turbulence of the flow is examined to notice the main energetic phenomena. This is done by displaying the turbulent kinetic energy downstream of the rotor column. Its values are given by the normalized formula :

$$k_{u_i u_j} = \frac{1}{2} \frac{\sigma(u_i^2) + \sigma(u_j^2)}{U_0^2} \tag{3}$$

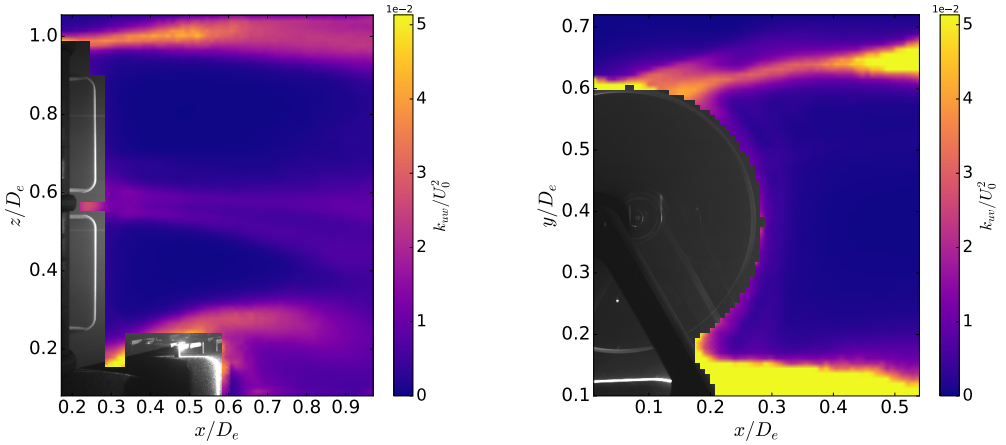

FIGURE 11 – Turbulent kinetic energy in the near wake of the rotor column. Rotors are hidden on the maps. Left : k_{uw} in the vertical plane at the half-width of the column. Right : k_{uv} in the horizontal plane at the half-height of the upper rotor.

The vertical plane (Fig. 11) primarily reveals high-energy components associated with the vertical U gradient which delimites the turbine's wake from the external region. The flow bypassing the foundation arm and the trace behind the middle plate are also highly energetic compared to the overall plane. Moreover, the horizontal plane shows high k_{uv} values behind the central pillar and along the contour of the lateral wake. The phenomena involved will be detailed in another study.

The section provides several insights into the flow behaviour in the near-machine region. The flow bypasses the top and sides of the machine, generating overspeed in the outer wake area. As the turbine captures energy from the flow, the near wake exhibits reduced velocity and is constrained by the entire machine geometry. It is now possible to investigate wake development in the far wake ($x/D_e \geq 1$).

V – Evolution of the flow in the far wake

Measurement tools make it possible to investigate the turbine's wake to further positions in the tank. The measurement planes were presented in section II – 3.

The wake development can be observed from the LDV measurements taken at various (x,y,z)-positions, as illustrated in Fig. 12. A notable aspect is the persistence of the flow overspeed around the wake, with streamwise velocity $\overline{U}$ reaching 1.15 to $1.20U_0$ outside the turbine's wake. This indicates a significant lateral blockage effect caused by the turbine within the tank. In fact, the machine's blockage within the tank is about 17%. The overspeed previously spotted in Fig. 10 above the machine is still visible, indicating its propagation in the upper part of the water column.

An asymmetry is observed in the wake of the single rotor column, whose development is influenced by the global geometry and the presence of the central pillar. Within the turbine's wake, a low-velocity region is noticed downstream of the rotor column, consistent with previous findings. By $x/D_e = 1.5$ the influence of the central pillar is no longer apparent, and the velocity deficit gradually decreases from $x/D_e = 2$. This conclusion is in line with [4], showing that the wake of two vertical axis rotors merge rapidly downstream of the turbine when blades move against the flow in the inner of the central pillar. In the (y,z) plane (Fig. 13), vortices are described by the vector field downstream each upper rotor, slightly shifted towards the outer wake. The three-dimensional nature of the wake is thus clearly visible for the upper rotors at both x-positions whereas it is less distinct for the lower stage, possibly due to constraints imposed by the foundation arms. These stationary vortices are characteristic of counter-rotating twin vertical axis systems, as observed experimentally by [9], their presence reflecting a gradual homogenisation of the flow in the wake.

Furthermore, the wake structure appears to maintain a consistent pattern downstream, though its dimensions change. From $x/D_e = 1$ to $x/D_e = 2.5$, the wake becomes homogenised, yet it retains a similar organisational structure.

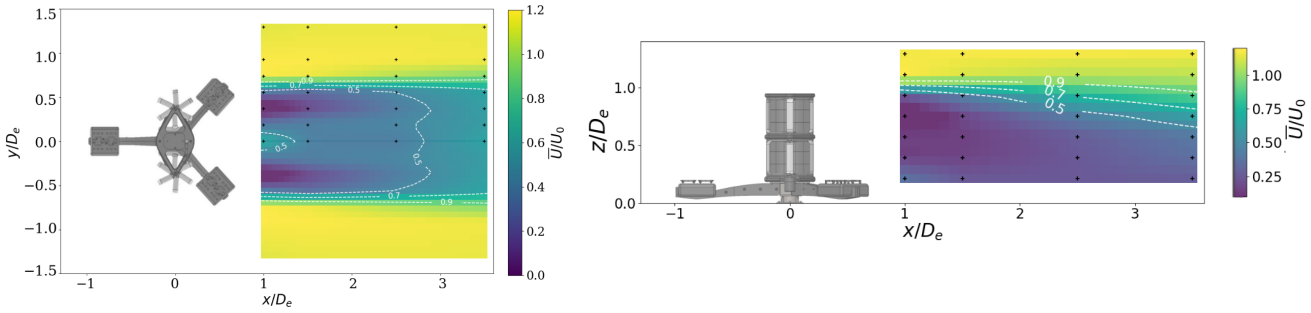

FIGURE 12 – LDV measurements in the far wake of the model. Left : [x,y] plane at mid-height upper rotors. Right : [x,z] plane at mid-width of the rotor column.

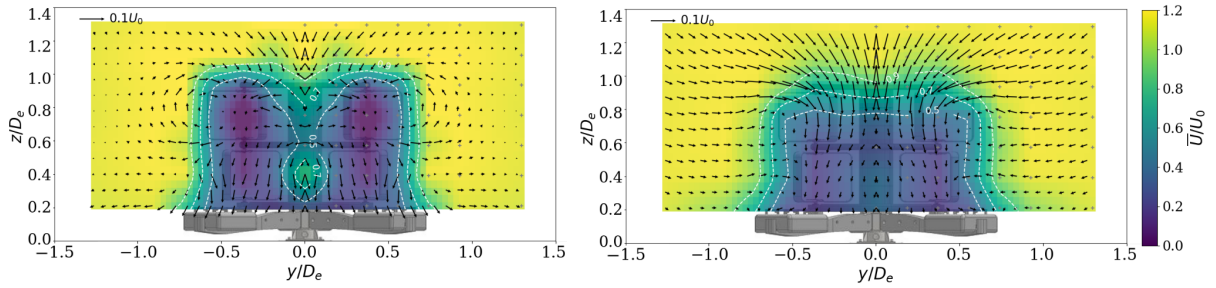

FIGURE 13 – LDV maps of the streamwise velocity component $\overline{U}$ in the wake of the model, at x/D_e=1 (left) and 2.5 (right).

In Fig. 14, the planes are used to determine the width and height of the wake at various x-positions. The wake is defined as the region where the mean velocity is less than $0.9U_0$. To determine the wake height at a given x-position, the average of the z-positions corresponding to the U = $0.9U_0$ contour is calculated, with y-values ranging from 0 to $w_m/2$, represented by the red zone in the figure. Similarly, to determine the half-width of the wake at a given x-position, the y-positions of the U = $0.9U_0$ outline are averaged for z ranging from 0 to h_m, corresponding to the blue zone in the figure. The blockage effect observed laterally should, however, be taken into account when considering

the width estimation. These parameters show that the height of the wake decreases with distance from the machine, as a 15% reduction in height is estimated from this technique. However, for the downstream studied positions, the width of the wake varies slightly, its estimation being virtually constant across all planes in this configuration. In addition, an interpolation method is proposed to evaluate the wake recovery length in Fig. 14 (right). The velocity is averaged over the rotors projected area (defined by $0 \leq y \leq w_m$ and on the height h_m), for each longitudinal position x. A linear trend is deduced from the curve, and its linear equation helps to find the distance for which $\overline{U} = 0.9U_0$. In this configuration at the optimum operating point, the condition is satisfied for $x = 9D_e$. This equivalent recovery length is typically obtained for vertical axis machines, both in the case of a single or two-columns interaction vertical axis [10], and in the case of a four-rotor structure [11]. This parameter can also be used in future studies to compare the wake evolution trends with other turbine configurations and technologies.

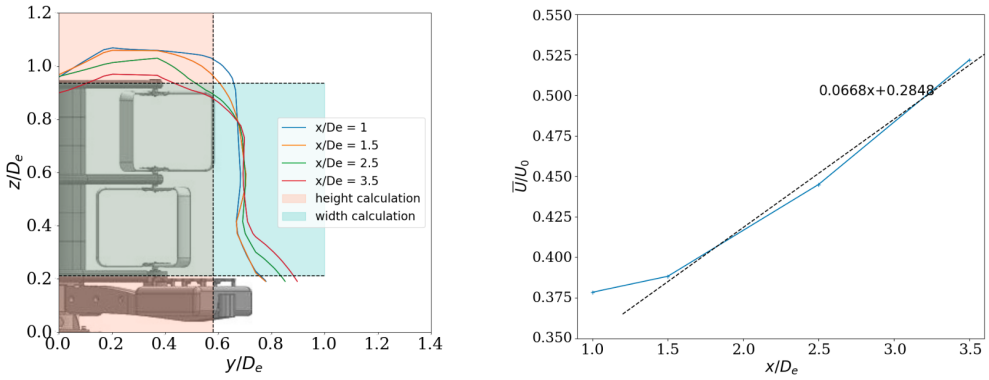

FIGURE 14 – Left : method to evaluate width and height of the turbine's wake at various x-positions. Right : estimation of the wake recovery length at the optimum operating point.

VI – Conclusions

The interaction between the flow and the OQ 2.5 turbine has been thoroughly investigated using LDV and PIV measurements conducted around the machine at its optimum operating point. The turbine significantly impacts the incident flow, as evidenced by the notable decrease in the streamwise component and the increased lateral flow velocity near the rotor. The turbine's structure affects the flow behaviour, the results confirming that the flow bypasses the top and sides of the turbine, generating overspeed regions outside the wake. In the near wake, the turbine's energy extraction results in a low-velocity area directly downstream of the rotor column, which gradually decreases with distance from the machine. The wake development includes a clear recirculating zone and swirling events behind the rotors, constrained by the machine's geometry. Energy distribution in the wake is mainly concentrated in two areas, in the U gradient (where energetic structures are emitted from the rotors and then propagating) and the model's geometry (foundation+ plates) influencing the flow behaviour. The width and height of the wake, determined from the velocity deficit zones, show that the wake first expands and dissipates as it moves downstream from the turbine, with very little lateral evolution.

Overall, the observations underline the importance of considering the turbine's induction effects and wake characteristics, as these effects are crucial for optimum turbines deployment and to ensure the structural integrity of the system. The flow behaviour must be faithfully reproduced in numerical models to ensure accurate predictions. However,

some limiting effects in the tank such as lateral blockage and Reynolds variation must be kept in mind to avoid misinterpreting these results. Comparing these results with tests on similar technologies could subsequently allow for the generalization of wake behaviour for vertical-axis machines within the test tank.

Acknowledgement

This work received the financial support of the French Agence Nationale de la recherche through the Verti-Lab project (ANR-23-LCV1-0009-01) and of the French Research and Technology National Association (ANRT) under the convention Cifre n° 2023/0217.
The authors acknowledge R. Linant, C. Penisson, JV. Facq and B. Gomez for their help during the experiments.

References

[1] L. Furgerot et al. "One year of measurements in Alderney Race : preliminary results from database analysis". In : *Philosophical Transactions of the Royal Society A : Mathematical, Physical and Engineering Sciences* 378 (2020).

[2] W. Batten et al. "The Prediction of the Hydrodynamic Performance of Marine Current Turbines". In : *Renewable Energy* 33 (2008), p. 1085-1096.

[3] X. Lin, J. Zhang et S. Liu. "Performance and wake interaction between two aligned vertical axis turbines". In : *Ocean Engineering* 292 (2024), p. 116478.

[4] S. Müller et al. "Experimental investigation of the wake characteristics behind twin vertical axis turbines". In : *Energy Conversion and Management* 247 (2021).

[5] S. Zanforlin, F. Burchi et N. Bitossi. "Hydrodynamic Interactions Between Three Closely-spaced Vertical Axis Tidal Turbines". In : *Energy Procedia* 101 (2016), p. 520-527.

[6] M. Grondeau et al. "Wake of a Ducted Vertical Axis Tidal Turbine in Turbulent Flows, LBM Actuator-Line Approach". In : *Energies* 12 (2019), p. 4273.

[7] M. Ikhennicheu et al. "Experimental study of coherent flow structures past a wall-mounted square cylinder". In : *Ocean Engineering* 182 (2019), p. 137-146.

[8] P. Ouro et T. Stoesser. "Wake Generated Downstream of a Vertical Axis Tidal Turbine". In : 2017.

[9] H. Lam et H. Peng. "Measurements of the wake characteristics of co- and counter-rotating twin H-rotor vertical axis wind turbines". In : *Energy* 131 (2017), p. 13-26. issn : 0360-5442.

[10] A. Vergaerde et al. "Experimental characterisation of the wake behind paired vertical-axis wind turbines". In : *Journal of Wind Engineering and Industrial Aerodynamics* 206 (2020), p. 104353. issn : 0167-6105.

[11] M. Moreau, G. Germain et G. Maurice. "Experimental performance and wake study of a ducted twin vertical axis turbine in ebb and flood tide currents at a 1/20th scale". In : *Renewable Energy* 214 (2023).